


## Thermal Resistance of GaN/AlN Graded Interfaces

Ambroise van Roieghem,<sup>1,\*</sup> Bjorn Vermeersch,<sup>1,†</sup> Jesús Carrete,<sup>2</sup> and Natalio Mingo<sup>1</sup>

<sup>1</sup>CEA, LITEN, 17 Rue des Martyrs, 38054 Grenoble, France

<sup>2</sup>Institute of Materials Chemistry, TU Wien, A-1060 Vienna, Austria

 (Received 28 September 2018; revised manuscript received 18 December 2018; published 14 March 2019)

Compositionally graded interfaces in power electronic devices eliminate dislocations but they can also decrease thermal conduction, leading to overheating. We quantify the thermal resistances of GaN/AlN graded interfaces of varying thickness using *ab initio* Green's functions and compare them with the abrupt interface case. A non-trivial power dependence of the thermal resistance versus the interface thickness emerges from the interplay of alloy and mismatch scattering mechanisms. We show that the overall behavior of such graded interfaces is very similar to that of a thin film of an effective alloy on the length scales relevant to real interfaces.

DOI: [10.1103/PhysRevApplied.11.034036](https://doi.org/10.1103/PhysRevApplied.11.034036)

### I. INTRODUCTION

The common strategy of interfacing two pure semiconductors via a gradual alloyed region poses a design trade-off: on the one hand, a thicker alloyed region is desirable in order to accommodate the lattice mismatch; on the other, a thick alloy will also negatively impact the thermal conductance across the interface, possibly degrading a device's lifetime. For example, common substrate designs for high-electron-mobility transistors (HEMTs) include a graded transition region between GaN and AlN as thick as  $1.5\ \mu\text{m}$  [1]. For substrates grown on Si, this region contributes only 3% of the total substrate thermal resistance. But if one replaces Si by diamond, the graded interface thermal resistance amounts to 20% of the total. For common operating conditions in HEMTs, this translates into a  $10^\circ$ – $20^\circ$  higher temperature of the active region, shortening the device's lifetime by one half [2].

Thus, it may pay off to try to make the graded region as thin as possible while still satisfying some minimum structural constraints. To do this, one needs to know how the interface thermal resistance depends on its thickness and composition profile. Theoretically quantifying it is, however, a nontrivial problem due to the simultaneous emergence of quasiballistic transport, wave interference effects, and the interplay between large-scale features and atomic-scale disorder. All this leads to a thermal resistance that no longer depends linearly on thickness when the latter gets below the  $\mu\text{m}$  range. Experimentally, one can only access the thermal conduction of the structure as a whole,

which typically includes many different material interfaces in a single sample. This makes it difficult to quantify the upper limits to the interface conductance based on experiments alone. It is therefore very important to theoretically predict the thermal conductance of graded interfaces, to know how much the grading strategy is degrading the performance of devices, and how much improvement could be achieved by other schemes, such as reducing the thickness or using digital structures. We tackle this question here for the technologically important case of GaN/AlN interfaces, which are ubiquitous in power electronics where thermal-dissipation issues are a major concern.

The use of graded interfaces to reduce threading dislocation density was theoretically tackled by Tersoff using an analytical model and has been deeply explored in subsequent modeling studies for two decades [3,4]. The specific grading length and profile to satisfy structural constraints (e.g., dislocation density or strain) depends on the particular problem in hand. The structural constraint aspect is not the goal of this paper and we refer the reader to earlier literature.

To model the thermal conductance of interfaces, mainstream techniques include the use of various phonon-gas models, such as the diffuse mismatch or acoustic mismatch models, atomistic Green's functions, or molecular dynamics [5–8]. A few theoretical studies have focused on trying to improve the interface thermal conductance between two different materials by using mass gradients [9]. However, in practice, the intermediate layers are often not perfectly ordered in the plane perpendicular to the interface but rather disordered alloys at a given composition. This is the case that we study here, using Monte Carlo simulations to account for the anharmonic and alloy scattering effects coupled to atomistic Green's functions

\*ambroise.van-roieghem@polytechnique.edu

†Current address: imec, Kapeldreef 75, 3001 Leuven, Belgium.

to compute the probability of transmission at the interface of two materials. We focus on the case of a very progressive step-graded interface and show that the total interface can be modeled as a thin film of an effective alloy, due to the dominant contribution from alloy scattering at realistic length scales. According to recent experimental results [7], the interface thermal resistance can actually be overestimated by atomistic Green's functions due to additional conductance from nonelastic processes, so this statement should be very robust in the case of those progressive interfaces of two similar crystal structures. We give a general expression for the characteristics of this effective alloy, such that the result can be easily applied to other interface profiles.

## II. METHODS

Current approaches to the atomistic investigation of interface thermal conductance are based on Green's functions [10–16]. However, when the interface is structurally complex or disordered in an extended region of space, as in the case of graded interfaces, it is impractical to simulate the whole atomically disordered interface. Doing so would require approximating the disordered interface by multiple realizations of exceedingly large supercells, periodic in the directions parallel to the interface [13]. A method to overcome this limitation was demonstrated in Refs. [17] and [18]. The basic idea is that the perturbation part of the Hamiltonian can be written as the sum of a contribution from the average perturbation over the layer (the “compositional profile” contribution) plus the local deviation with respect to this average for each atom (the “disorder” contribution). The total phonon-scattering intensity is the sum of the scattering intensities of each of the two contributions separately, plus the interference term between them, which is neglected on the grounds of phase cancellation due to disorder. The “compositional profile” scattering term preserves the phonon quasimomentum component parallel to the interface and can be efficiently calculated using atomistic Green's functions. The “disorder” term does not preserve quasimomentum and it is computed within the framework of the virtual crystal approximation. Using realistic compositional profiles and *ab initio* calculated force constants, a good agreement with experiment is obtained for superlattices with periods comprising up to 45 atomic layers, without the use of any adjustable parameters [17,18].

The approach implemented for superlattices is not directly applicable to single interfaces and requires modification. The difference comes from the periodic character of the superlattices, versus the local and asymmetric character of the single interface. The repeated structure of the superlattices justifies a picture in which phonons travel in an effective medium and are incoherently scattered by the homogeneously distributed changes in composition.

The T-matrix formalism is best suited to this problem. In contrast, the materials at each side of the single interface are dissimilar and thus cannot be treated by the T-matrix formulation of Refs. [17], [19], and [20], which requires having the same material infinitely far from the interface on either side. Instead, the Green's function formalism for transmission and reflection probabilities is used here [10,11].

In the considered geometry, the interface is bidimensional and infinite in two directions, so that a transmission or a reflection event will conserve the component of momentum parallel to the interface as well as the energy. The dynamical matrix of each bulk material, calculated *ab initio*, is first Fourier transformed in the direction perpendicular to the interface to obtain a set of mixed-space force constants:

$$\tilde{\Phi}_{\alpha i}^{\alpha' i'}(q_{\parallel}, X_m) = \sum_{n < N} \sqrt{M_{\alpha} M_{\alpha'}} D_{\alpha i}^{\alpha' i'}(\mathbf{q}_{\parallel} + \mathbf{q}_{\perp n}) e^{-iq_{\perp n} X_m}, \quad (1)$$

where  $N$  is the chosen number of samples over the Brillouin zone in the direction perpendicular to the interface,  $\alpha$  and  $\alpha'$  are the indexes over atoms,  $i$  and  $i'$  those over the Cartesian directions,  $D$  is the dynamical matrix, and the  $M$  are the masses of the atomic species. The  $X_{m < N}$  are lattice vectors perpendicular to the interface and  $\tilde{\Phi}_{\alpha i}^{\alpha' i'}(\mathbf{q}_{\parallel}, X_m)$  corresponds to the interactions between layers separated by  $X_m$  in real space for a given parallel wave vector.

Using this set of force constants, the two-dimensional Green's function  $g(\mathbf{q}_{\parallel})$  of each material is computed using the decimation technique [21,22]. The interactions  $k_{12}(\mathbf{q}_{\parallel})$  between layers of different materials 1 and 2 in real space are obtained from the averaged mixed-space force constants and using the masses of the two different materials. For  $\mathbf{q}_{\parallel} = 0$ , the acoustic sum rule is enforced by correcting the values of the diagonal elements. Finally, we obtain the transmission between the two materials using the two-region formula [10,11], for each parallel wave vector:

$$T = 4\pi^2 \text{Tr}[\rho_1 D_1^A k_{12} \rho_2 D_2^R k_{21}] \quad (2)$$

where  $D_1^A = (I - k_{12} g_2^+ k_{21} g_1^+)^{-1}$ ,  $D_2^R = (I - k_{21} g_1 k_{12} g_2)^{-1}$ , and  $2\pi\rho = g - g^+$  is the spectral density of states of the decoupled system.

This transmission is subsequently used within the Monte Carlo solver implemented in ALMABTE [23]. The *ab initio* data for GaN and AlN has been computed in a  $5 \times 5 \times 5$  supercell within the local density approximation of density functional theory, and can be retrieved from the database on the ALMABTE website. For each incoming mode, only outgoing modes that conserve the parallel wave vector and the frequency are considered (for transmission or reflection). When several outgoing modes are available for one

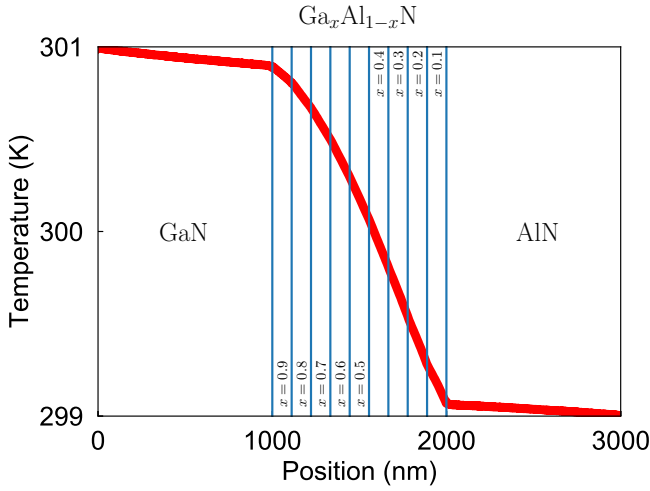


FIG. 1. The structure of the considered GaN/AlN (001) step-graded interfaces and associated temperature profile (here, the total length of the interface is 999 nm).

incoming mode, their probability is weighted by their group velocity projected on the normal to the interface.

One difficulty in simulating a step-graded interface is to combine this mismatch scattering with the intrinsic scattering from the alloy disorder within the layers. To tackle this issue, we choose to slice the interface into steps with gradual increases in composition of 10% (see Fig. 1). In the limit of very short interfaces, mismatch scattering becomes dominant, while if the interface is very thick, alloy scattering takes over.

Finally, the interface thermal resistance is evaluated from the temperature profiles and heat fluxes obtained from the Monte Carlo simulation, using buffer layers of  $1 \mu\text{m}$  at each side of the interface, as follows:

$$R = \Delta T/J, \quad (3)$$

where  $J$  represents the total heat flux across the structure and  $\Delta T$  is the jump in temperature across the interface.

### III. THERMAL RESISTANCES OF GAN/ALN STEP-GRADED INTERFACES

In the following, we focus on step-graded interfaces from GaN to AlN, oriented along the (001) direction. All properties are computed *ab initio*, using a  $15 \times 15 \times 15$  grid for the phonon wave vectors and 15 samples for the mixed-space force constants.

In Fig. 1, we display the temperature profile obtained for a step-graded interface of about  $1 \mu\text{m}$ . As can be seen from the absence of temperature jumps, the effect of the successive interfaces on the thermal resistance is negligible compared to the scattering from alloy disorder. In this context, one can model the step-graded structure as an

effective alloy in which the mass-disorder scattering contribution is similar to that of an alloy with concentration  $\text{Ga}_{\tilde{x}}\text{Al}_{1-\tilde{x}}\text{N}$ , such that

$$\tilde{x}(1 - \tilde{x}) = \frac{1}{N} \sum_{i < N} x_i(1 - x_i), \quad (4)$$

where  $x_i$  the concentration in each layer of the alloy. A similar approach has been shown to give excellent results in the context of superlattices [18]. Here,  $\tilde{x} \simeq 0.24$  and in the continuous limit  $\tilde{x} = 1/2 - \sqrt{3}/6$ . At the same time, the phonon spectrum, average masses, and three-phonon properties of this effective alloy correspond to those of the average alloy (here, with concentration  $\text{Ga}_{0.5}\text{Al}_{0.5}\text{N}$ ). Finally, the finite length of the interface limits the mean free path of the phonons, as described in Ref. [24]:

$$\frac{1}{R} = \sum_{v_{\perp}(q) > 0} \frac{C(q)v_{\perp}(q)\Lambda_{\perp}(q)}{L + 2\Lambda_{\perp}(q)}, \quad (5)$$

where  $R$  is the thermal resistance of the interface of length  $L$ ,  $C$  is the specific heat of a phonon mode, and  $v_{\perp}$  and  $\Lambda_{\perp}$  are, respectively, its group velocity and mean free path projected on the normal to the interface. As shown in Fig. 2, such an approximation gives excellent results in the range of lengths applicable to real interfaces, from nanometer to micrometer scales. We also observe, in the lower panel, a power law similar to the one found for (Al,Ga)N alloy thin films [24].

In the limit of an infinitely long interface, the resistance should follow an asymptotic trend equal to the total length divided by the average of the bulk conductivities of the different alloys, here  $25.9 \text{ W}/(\text{m K})$  compared to the bulk conductivity of the effective alloy of  $22.8 \text{ W}/(\text{m K})$ . In the limit of an infinitely thin interface, the conductivity becomes limited by the transmission probability and the resistance of an abrupt interface is computed to be  $2 \text{ m}^2 \text{ K}/\text{GW}$ . In contrast, a step-graded interface of  $9 \text{ nm}$  already has a resistance of  $3.4 \text{ m}^2 \text{ K}/\text{GW}$ , showing that the alloy scattering will start to dominate for longer interfaces. Interestingly, this latter value is very much in line with the resistance of the effective alloy (see the middle panel of Fig. 2). Indeed, at these small length scales, the resistance originating from mismatch scattering is partially compensated by a lowering of the resistance caused by alloy scattering, due to the simultaneous filtering of phonon modes at the successive interfaces.

This effect is illustrated in Fig. 3, which displays the energy-resolved spectral heat flux of a structure including a GaN/AlN (001) step-graded interface of  $90 \text{ nm}$ . The successive interfaces are very transparent to the main conduction channels at low energies, while the alloy scattering strongly limits the mean free path of the optical modes around  $50 \text{ rad}/\text{ps}$  compared to the pure materials. The

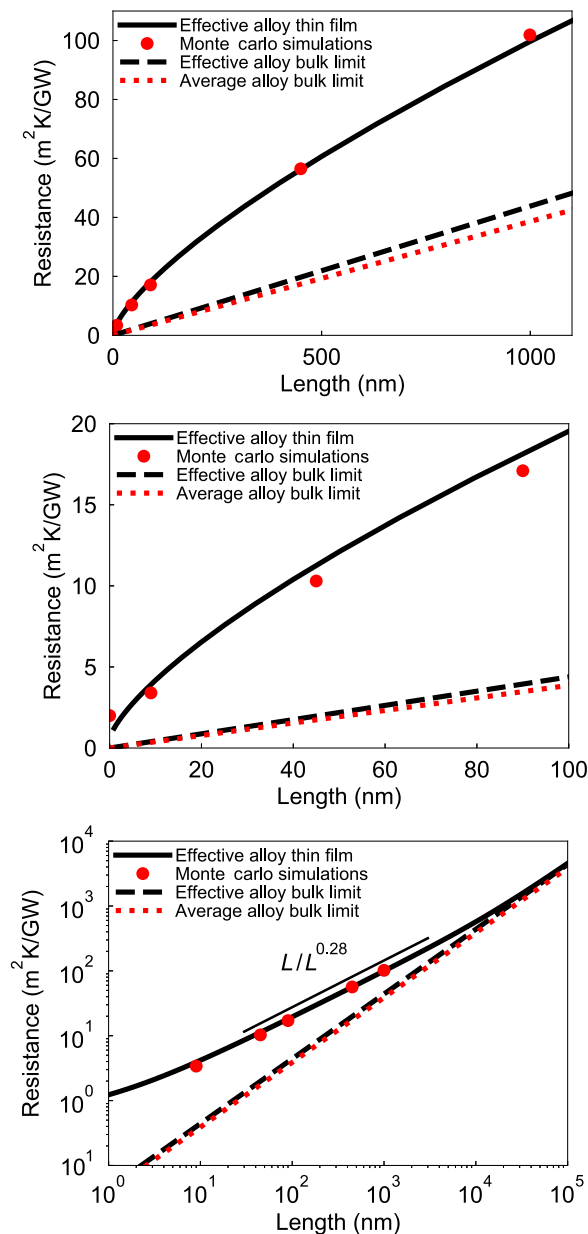


FIG. 2. The resistances of GaN/AlN (001) step-graded interfaces of different lengths as computed from Monte Carlo simulations, compared with the resistance of the effective alloy thin film and with the bulk effective alloy and average alloy limits. Upper panel, the full data; middle panel, zoom at short lengths; lower panel, the data on a log-log scale to demonstrate the effective power law for the interface resistance.

high-frequency features above 100 rad/ps are due to the redistribution of phonon population, since their mean free path is barely impacted by alloy scattering compared to the aforementioned modes around 50 rad/ps. This is due to the different character of those modes: the alloy scattering rates computed within the Tamura formula [25] are linked to the density of states of Ga/Al character, while the highest modes are mostly of N character, as pointed

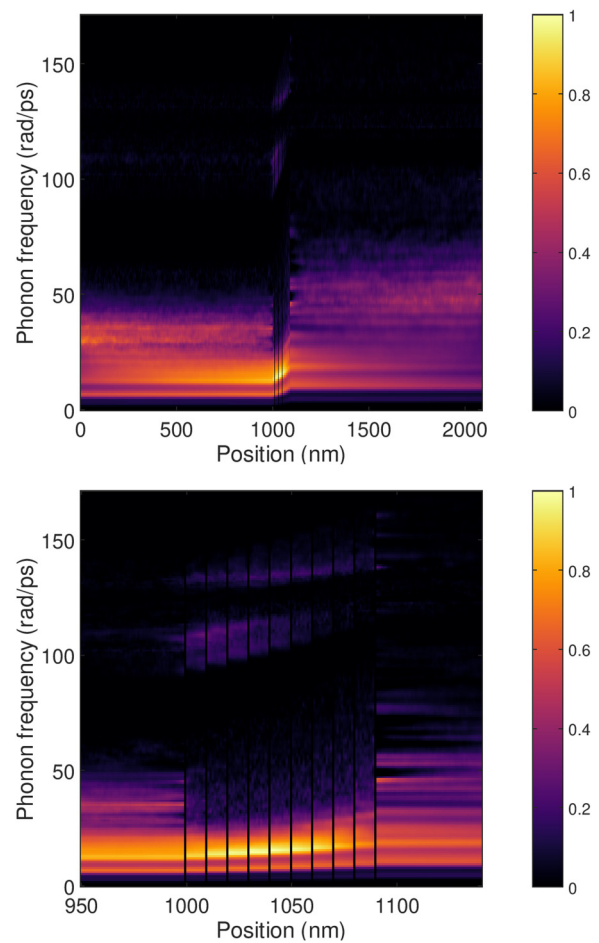


FIG. 3. The energy-resolved spectral heat flux in a GaN/AlN (001) step-graded interface of 90 nm, as computed from Monte Carlo simulations. Upper panel, full structure including the buffer layers; lower panel, a zoom close to the interface. The spectral heat flux has been normalized to its maximum value,  $3.4 \mu\text{J}/(\text{m}^2 \text{ rad})$ .

out in the case of InN by Polanco and Lindsay [26]. In the framework of the Monte Carlo solver within the relaxation time approximation, the flux is thus redistributed proportionally more in those modes in the alloys than in the pure compounds.

#### IV. OPTIMIZING THE THERMAL CONDUCTANCE IN REAL DEVICES

We now discuss the potential optimization of such interfaces. On the one hand, making the graded interface thicker lowers the density of threading dislocations. This improves overall performance in a device-dependent fashion that can be complex to quantify. On the other hand, thicker interfaces can also reduce performance because of device heating resulting from an increased thermal resistance. The balance between these counteracting effects will lead to an optimal grading thickness, which should be



optimized on a case-by-case basis for each device. Some current devices are grown on silicon substrate that can be 1000  $\mu\text{m}$  thick, which adds a thermal resistance of approximately 7700  $\text{m}^2 \text{K/GW}$ . In such cases, the device thermal resistance is dominated by the substrate, making it advantageous to have thick graded regions, since the gain in electrical performance by reducing dislocations is greater than the thermal penalty that they contribute.

The picture is very different, however, if a good thermally conducting substrate is employed. For example, the thermal conductivity of diamond is 17 times higher than that of silicon, translating into an approximately 450  $\text{m}^2 \text{K/GW}$  thermal resistance for a thickness of 1000  $\mu\text{m}$ . As Fig. 2 shows, in this case the resistance contributed by the graded interfaces in the device would already be a non-negligible part of the total. A difficulty in making good conducting substrates is related to the thermal resistance of the bonding between the substrate and the device. However, very low thermal resistances have recently been achieved for diamond/GaN and SiC/GaN, of 36 and 4.1  $\text{m}^2 \text{K/GW}$ , respectively [27–29]. On such new-generation substrates, it can pay off to reduce the thickness of the graded regions to some extent, at the expense of an increased dislocation density, to decrease overheating and enhance efficiency and device lifetime.

An increased dislocation density can also lead to increased thermal resistance. However, *ab initio* calculations and analysis of experimental data indicate that, for dislocation densities under  $1 \times 10^{10} \text{ cm}^{-2}$ , the thermal conductivity reduction in GaN due to dislocations is minimal and has been overshadowed by thin-film effects in previous experiments [30]. The threading dislocation density in GaN directly grown on sapphire, SiC, or Si(111), is typically between  $1 \times 10^8$  and  $1 \times 10^{10} \text{ cm}^{-2}$  [31].

The mean time to failure (MTF) of a device is affected by different mechanisms and its temperature dependence depends on the particular device in under consideration [32–35]. Common temperature dependencies of GaN device MTFs follow exponential behaviors and may decrease by one order of magnitude for every roughly 50  $^\circ\text{C}$  increase in the temperature of the active region. The operating temperature of HEMTs can reach well above 100  $^\circ\text{C}$ . In the well-bonded diamond substrate case above, the over 20% thermal resistance contributed by a 1- $\mu\text{m}$ -thick graded interface may thus lead to overheating by 20  $^\circ\text{C}$  and shorten the device’s MTF by half.

## V. CONCLUSION

Using an *ab initio* Green’s function approach, we compute the lattice thermal resistances of a series of GaN/AIN (001) step-graded interfaces of different lengths. We find that mismatch scattering is very weak in the main conduction channels, such that alloy scattering becomes dominant

in the regime relevant for real interfaces (10 nm to 1  $\mu\text{m}$ ). The computed resistance of the step-graded interface is well approximated by that of a model thin film of an effective alloy and it strongly deviates from the classical Fourier-law predictions. The resistance of 1- $\mu\text{m}$ - and 100-nm-thick interfaces exceeds conventional estimates by factors of 2 and 4, respectively. In the case of well-sunk devices, graded interfaces add a non-negligible contribution to overheating and it can be advisable to shorten the thickness of the step-graded interfaces at the expense of a larger density of threading dislocations. The thermal resistances calculated in this paper represent valuable information for the optimization of GaN-based power-electronic devices.

## ACKNOWLEDGMENTS

We acknowledge support from the European Union’s Horizon 2020 Framework Programme for Research and Innovation, Grant No. 645776 (ALMA). We thank C. Giesen for sharing thickness data from real substrates.

- 
- [1] C. Giesen (private communication).
  - [2] Assuming 1000  $\mu\text{m}$  of Si or diamond and 7 W/(mK) for the graded region.
  - [3] J. Tersoff, Dislocations and strain relief in compositionally graded layers, *Appl. Phys. Lett.* **62**, 693 (1993).
  - [4] B. Bertoli, E. N. Suarez, J. E. Ayers, and F. C. Jain, Misfit dislocation density and strain relaxation in graded semiconductor heterostructures with arbitrary composition profiles, *J. Appl. Phys.* **106**, 073519 (2009).
  - [5] E. T. Swartz and R. O. Pohl, Thermal boundary resistance, *Rev. Mod. Phys.* **61**, 605 (1989).
  - [6] Zhi Liang, Kiran Sasikumar, and Pawel Keblinski, Thermal Transport Across a Substrate–Thin-Film Interface: Effects of Film Thickness and Surface Roughness, *Phys. Rev. Lett.* **113**, 065901 (2014).
  - [7] John T. Gaskins, George Kotsonis, Ashutosh Giri, Shenghong Ju, Andrew Rohskopf, Yekan Wang, Tingyu Bai, Edward Sachet, Christopher T. Shelton, Zeyu Liu, Zhe Cheng, Brian M. Foley, Samuel Graham, Tengfei Luo, Asegun Henry, Mark S. Goorsky, Junichiro Shiomi, Jon-Paul Maria, and Patrick E. Hopkins, Thermal boundary conductance across heteroepitaxial ZnO/GaN interfaces: Assessment of the phonon gas model, *Nano. Lett.* **18**, 7469 (2018).
  - [8] Zhun-Yong Ong, Tutorial: Concepts and numerical techniques for modeling individual phonon transmission at interfaces, *J. Appl. Phys.* **124**, 151101 (2018).
  - [9] Yanguang Zhou, Xiaoliang Zhang, and Ming Hu, An excellent candidate for largely reducing interfacial thermal resistance: A nano-confined mass graded interface, *J. Nanoscale* **8**, 1994 (2016).
  - [10] N. Mingo and Liu Yang, Phonon transport in nanowires coated with an amorphous material: An atomistic Green’s function approach, *Phys. Rev. B* **68**, 245406 (2003).

- [11] Natalio Mingo, Green's function methods for phonon transport through nano-contacts, *Therm. Nanosyst. Nanomater.* **118**, 63 (2009).
- [12] Zhun-Yong Ong and Gang Zhang, Efficient approach for modeling phonon transmission probability in nanoscale interfacial thermal transport, *Phys. Rev. B* **91**, 174302 (2015).
- [13] Zhiting Tian, Keivan Esfarjani, and Gang Chen, Green's function studies of phonon transport across Si/Ge superlattices, *Phys. Rev. B* **89**, 235307 (2014).
- [14] J.-S. Wang, J. Wang, and J. T. Lü, Quantum thermal transport in nanostructures, *Eur. Phys. J. B* **62**, 381 (2008).
- [15] W. Zhang, N. Mingo, and T. S. Fisher, Simulation of phonon transport across a non-polar nanowire junction using an atomistic Green's function method, *Phys. Rev. B* **76**, 195429 (2007).
- [16] W. Zhang, T. S. Fisher, and N. Mingo, The atomistic Green's function method: An efficient simulation approach for nanoscale phonon transport, *Numer. Heat Transf., Part B: Fundam.* **51**, 333 (2010).
- [17] Peixuan Chen, N. A. Katcho, J. P. Feser, Wu Li, M. Glaser, O. G. Schmidt, David G. Cahill, N. Mingo, and A. Rastelli, Role of Surface-Segregation-Driven Intermixing on the Thermal Transport through Planar Si/Ge Superlattices, *Phys. Rev. Lett.* **111**, 115901 (2013).
- [18] J. Carrete, B. Vermeersch, L. Thumfart, R. R. Kakodkar, G. Trevisi, P. Frigeri, L. Seravalli, J. P. Feser, A. Rastelli, and N. Mingo, Predictive design and experimental realization of InAs/GaAs superlattices with tailored thermal conductivity, *J. Phys. Chem. C* **122**, 4054 (2018).
- [19] N. Mingo, D. A. Stewart, D. A. Broido, L. Lindsay, and W. Li, in *Length-Scale Dependent Phonon Interactions*, edited by Subhash L. Shinde and Gyaneshwar P. Srivastava, Topics in Applied Physics Vol. 128 (Springer, New York, 2014), p. 137.
- [20] Nakib Haider Protik, Jesús Carrete, Nebil A. Katcho, Natalio Mingo, and David Broido, *Ab initio* study of the effect of vacancies on the thermal conductivity of boron arsenide, *Phys. Rev. B* **94**, 045207 (2016).
- [21] F. Guinea, C. Tejedor, F. Flores, and E. Louis, Effective two-dimensional Hamiltonian at surfaces, *Phys. Rev. B* **28**, 4397 (1983).
- [22] M. P. Lopez Sancho, J. M. Lopez Sancho, J. M. L. Sancho, and J. Rubio, Highly convergent schemes for the calculation of bulk and surface Green functions, *J. Phys. F: Metal Phys.* **15**, 851 (1985).
- [23] Jesús Carrete, Bjorn Vermeersch, Ankita Katre, Ambrose van Roekeghem, Tao Wang, Georg K. H. Madsen, and Natalio Mingo, ALMABTE: A solver of the space-time dependent Boltzmann transport equation for phonons in structured materials, *Comput. Phys. Commun.* **220**, 351 (2017).
- [24] Bjorn Vermeersch, Jesús Carrete, and Natalio Mingo, Cross-plane heat conduction in thin films with *ab-initio* phonon dispersions and scatter ingrates, *Appl. Phys. Lett.* **108**, 193104 (2016).
- [25] Shin-ichiro Tamura, Isotope scattering of large-wave-vector phonons in GaAs and INSB: Deformation-dipole and overlap-shell models, *Phys. Rev. B* **30**, 849 (1984).
- [26] Carlos A. Polanco and Lucas Lindsay, Thermal conductivity of InN with point defects from first principles, *Phys. Rev. B* **98**, 014306 (2018).
- [27] Jungwan Cho, E. Bozorg-Grayeli, D. H. Altman, Mehdi Asheghi, and Kenneth E. Goodson, Low thermal resistances at GaN–SiC interfaces for HEMT technology, *IEEE Electron Device Lett.* **33**, 378 (2012).
- [28] Jungwan Cho, Zijian Li, E. Bozorg-Grayeli, T. Kodama, D. Francis, F. Ejeckam, F. Faili, M. Asheghi, and K. E. Goodson, Improved thermal interfaces of GaN-diamond composite substrates for HEMT applications, *IEEE Trans. Compon., Packag. Manuf. Technol.* **3**, 79 (2013).
- [29] Robert M. Radway, PhD thesis, Massachusetts Institute of Technology, 2017.
- [30] T. Wang, J. Carrete, N. Mingo, and G. K. H. Madsen, Phonon scattering by dislocations in GaN, *ACS Appl. Mater. Interfaces* **11**, 8175 (2019).
- [31] Carol I. H. Ashby, Christine C. Mitchell, Jung Han, Nancy A. Missert, Paula P. Provencio, David M. Follstaedt, Gregory M. Peake, and Leonardo Griego, Low-dislocation-density GaN from a single growth on a textured substrate, *Appl. Phys. Lett.* **77**, 3233 (2000).
- [32] S. D. Burnham, R. Bowen, J. Tai, D. Brown, R. Grabar, D. Santos, J. Magadia, I. Khalaf, and M. Micovic, Reliability characteristics and mechanisms of HRL's T3 GaN technology, *IEEE Trans. Semicond. Manuf.* **30**, 480 (2017).
- [33] David Cheney, Erica Douglas, Lu Liu, Chien-Fong Lo, Brent Gila, Fan Ren, Stephen Pearton, David J. Cheney, Erica A. Douglas, Lu Liu, Chien-Fong Lo, Brent P. Gila, Fan Ren, and Stephen J. Pearton, Degradation mechanisms for GaN and GaAs high speed transistors, *Materials* **5**, 2498 (2012).
- [34] Huarui Sun, Miguel Montes Bajo, Michael J. Uren, and Martin Kuball, Progressive failure site generation in a GaN/GaN high electron mobility transistors under OFF-state stress: Weibull statistics and temperature dependence, *Appl. Phys. Lett.* **106**, 043505 (2015).
- [35] R. Coffie, Y. Chen, I. P. Smorchkova, B. Heying, V. Gambin, W. Sutton, Y. Chou, W. Luo, M. Wojtowicz, and A. Oki, in *2007 IEEE International Reliability Physics Symposium Proceedings. 45th Annual* (IEEE, New York, NY, USA, 2007), p. 568.